

Synthesis and stability of hydrogen selenide compounds at high pressure

Cite as: *J. Chem. Phys.* **147**, 184303 (2017); <https://doi.org/10.1063/1.5004242>

Submitted: 12 September 2017 . Accepted: 24 October 2017 . Published Online: 13 November 2017

Edward J. Pace, Jack Binns, Miriam Peña Alvarez, Philip Dalladay-Simpson, Eugene Gregoryanz, and Ross T. Howie



[View Online](#)



[Export Citation](#)



[CrossMark](#)

ARTICLES YOU MAY BE INTERESTED IN

[High pressure synthesis and stability of cobalt hydrides](#)

The Journal of Chemical Physics **148**, 144310 (2018); <https://doi.org/10.1063/1.5026535>

[The metallization and superconductivity of dense hydrogen sulfide](#)

The Journal of Chemical Physics **140**, 174712 (2014); <https://doi.org/10.1063/1.4874158>

[Pressure calibration of diamond anvil Raman gauge to 310GPa](#)

Journal of Applied Physics **100**, 043516 (2006); <https://doi.org/10.1063/1.2335683>

Lock-in Amplifiers
[Find out more today](#)



 **Zurich Instruments**

Synthesis and stability of hydrogen selenide compounds at high pressure

Edward J. Pace,¹ Jack Binns,² Miriam Peña Alvarez,³ Philip Dalladay-Simpson,² Eugene Gregoryanz,^{2,3} and Ross T. Howie^{2,a)}

¹School of Chemistry and Centre for Science at Extreme Conditions, University of Edinburgh, Edinburgh EH9 3FD, United Kingdom

²Center for High Pressure Science and Technology Advanced Research, 1690 Cailun Rd., Building 6, Pudong, Shanghai 201203, People's Republic of China

³School of Physics and Astronomy and Centre for Science at Extreme Conditions, University of Edinburgh, Edinburgh EH9 3FD, United Kingdom

(Received 12 September 2017; accepted 24 October 2017; published online 13 November 2017)

The observation of high-temperature superconductivity in hydride sulfide (H_2S) at high pressures has generated considerable interest in compressed hydrogen-rich compounds. High-pressure hydrogen selenide (H_2Se) has also been predicted to be superconducting at high temperatures; however, its behaviour and stability upon compression remains unknown. In this study, we synthesize H_2Se *in situ* from elemental Se and molecular H_2 at pressures of 0.4 GPa and temperatures of 473 K. On compression at 300 K, we observe the high-pressure solid phase sequence (I-I'-IV) of H_2Se through Raman spectroscopy and x-ray diffraction measurements, before dissociation into its constituent elements. Through the compression of H_2Se in H_2 media, we also observe the formation of a host-guest structure, $(H_2Se)_2H_2$, which is stable at the same conditions as H_2Se , with respect to decomposition. These measurements show that the behaviour of H_2Se is remarkably similar to that of H_2S and provides further understanding of the hydrogen chalcogenides under pressure. *Published by AIP Publishing.*

<https://doi.org/10.1063/1.5004242>

I. INTRODUCTION

The recent claim of high-temperature superconductivity in hydrogen sulfide at megabar pressures has drawn attention back to the formation of hydrides with exotic properties.¹ The superconductive mechanism, composition, structure, and stability field of sulfur hydride at high pressures have been extensively investigated, although decisive conclusions have yet to be reached.^{2–10} Despite this interest and predictions of high T_c superconductivity, the heavier hydrogen chalcogenides (i.e., H_2Se and H_2Te) remain experimentally unexplored.^{11,12}

H_2Se is known to form from the direct reaction between Se and H_2 at high temperature. However, experimental studies of the solid state are limited to ambient pressure, low temperature investigations.^{13–16} As the heavier sister molecule to hydrogen sulfide, hydrogen selenide is likely to exhibit similar behaviour at high pressure; indeed, theoretical studies at the megabar regime find similarities in the solid phases.^{11,17}

H_2S exhibits three solid phases between pressures of 0.5 GPa and 27 GPa at 300 K: transitioning from a rotationally disordered solid (I-I') to an ordered hydrogen-bonded structure (IV), before dissociating.^{18–26} To date, there have been no experimental high-pressure investigations of H_2Se , but low temperature studies at ambient pressure find strong similarities in the crystal structures and Raman characteristics of phases

I–III, with their corresponding phases in H_2S .^{14,16} Mixtures of H_2S and H_2 are known to form $(H_2S)_2H_2$, a host-guest compound at pressures as low as 3.5 GPa.²⁷ High T_c superconductivity has been predicted in high-pressure simulations of both H_2S and $(H_2S)_2H_2$ compounds.^{28,29} Combined experimental and theoretical efforts have suggested the high- T_c phase as an H_3S compound, with a maximum T_c of 203 K at 155 GPa.^{1,8,29} With Se being larger and slightly less electronegative, computational studies predict lower stability with respect to pressure but propose the formation of superconducting phases H_3Se and HSe above \sim 120 GPa, with maximum T_c estimated between 110 and 130 K.^{11,17} To further understand the predicted exotic phenomena, it is important to first investigate the formation and high-pressure stability of H_2Se and to compare the behaviour with that of the extensively studied H_2S .

In this study, we report the direct synthesis of H_2Se from its constituent elements at conditions of 0.4 GPa and \sim 473 K. We find that phase I of H_2Se undergoes a phase transition at 12 GPa, similar to the transition to phase IV in H_2S . In H_2 -rich mixtures, we observe the formation of a host-guest $(H_2Se)_2H_2$ structure above 4.2 GPa. This compound is identified by characteristic vibrational Raman spectra differing from pure H_2Se . The structure and stoichiometry of this compound were confirmed through x-ray diffraction measurements whereby we find $(H_2Se)_2H_2$ to crystallize in a body-centered tetragonal structure, space group $I4/mcm$, analogous to that observed in $(H_2S)_2H_2$. Both H_2Se and $(H_2Se)_2H_2$ are stable to 24 GPa at 300 K, after which both decompose into their constituent elements.

^{a)}Email: ross.howie@hpstar.ac.cn

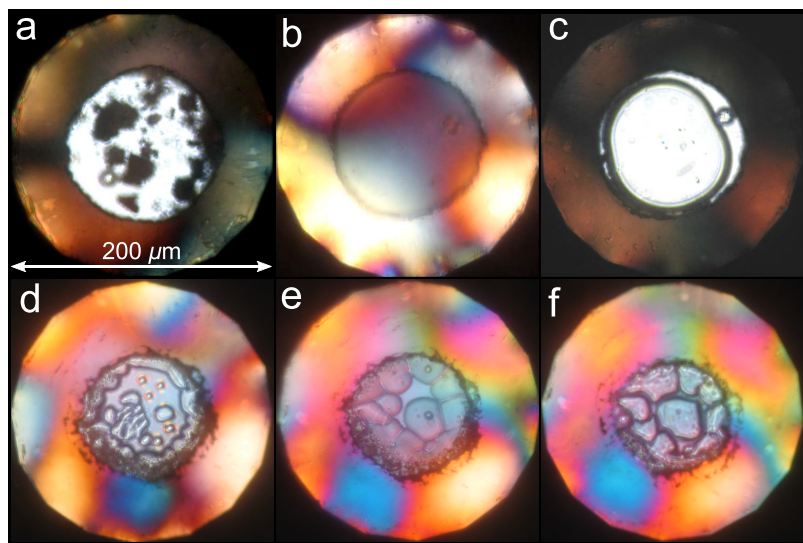


FIG. 1. Photomicrographs of the synthesis of H_2Se in a diamond-anvil cell sample chamber. The sample chamber is formed by a rhenium gasket. (a) H_2 and solid Se at 0.4 GPa and room temperature, (b) $\text{H}_2\text{Se}-\text{H}_2$ mixture at 0.4 GPa and 473 K, (c) liquid phase separation of H_2Se (central bubble) and H_2 (surrounding area) at 0.4 GPa and room temperature after heating, (d) H_2Se beginning to solidify, (e) slow coalescence of H_2Se regions, (f) completely solidified H_2Se at 1.5 GPa.

II. EXPERIMENTAL DETAILS

At ambient condition, H_2Se is a highly toxic and flammable gas. Such hazards can be avoided by the direct synthesis of H_2Se from Se and fluid H_2 in a diamond-anvil cell. Moreover, this technique also allows precise control of the ratio of H_2Se to H_2 . High purity selenium (99.999%) was loaded into a diamond-anvil cell with a small chip of ruby and subsequently gas loaded with research grade hydrogen (99.9999%) at 0.2 GPa [Fig. 1(a)].³⁰ Rhenium gaskets were used to form the sample chamber in all experimental runs. Sample sizes ranged between 100 and 125 μm once in the solid state. Once loaded, Se– H_2 mixtures were then compressed to 0.4 GPa and heated to 473 K for at least 2 h until all the Se had reacted [Fig. 1(b)]. On slowly cooling to room temperature, liquid H_2Se was obtained with clear phase separation from fluid H_2 as a consequence of non-stoichiometry [Fig. 1(c)]. We found that heating was necessary to promote the reaction of Se and H_2 . Leaving Se– H_2 mixtures at pressures between 0.2 GPa and 3 GPa for one month did not promote synthesis at room temperature.

H_2Se is very sensitive to both laser light and x-ray synchrotron radiation, which causes the sample to decompose, therefore precautions were required during data acquisition. Raman spectroscopy measurements were made using a custom-built micro-focused Raman system.^{31,32} The laser power of the system was kept below 10 mW to prevent decomposition of the sample to Se and H_2 . We have found that 647 nm laser emission was favorable over shorter wavelengths and did not cause any degradation of the sample during data acquisition. We found that the sample in the liquid state was much more prone to laser damage; thus, measurements were collected above pressures of 3.8 GPa. X-ray diffraction data were collected at beamline 16-IDB at the Advanced Photon Source (USA). Angle-dispersive x-ray diffraction patterns were recorded on a Pilatus 1M-F image-plate detector with a micro-focused synchrotron radiation of 30 keV. Data were integrated with DIOPTAS³³ to yield intensity vs. 2θ plots. Patterns were indexed with GSAS-II,³⁴ and Le Bail³⁵ refinements were carried out in JANA2006.³⁶ Exposure

of H_2Se to synchrotron x-ray radiation resulted in the formation of amorphous Se at the point of exposure, requiring the acquisition of data from a different sample position at each pressure point. Powder quality was very poor in all samples excluding the possibility of Rietveld profile refinement.

III. RESULTS AND DISCUSSION

On compression above 1 GPa, H_2Se began to nucleate in fluid H_2 [see Figs. 1(d)–1(f)] with full crystallization occurring at pressures of 1.5 GPa [Fig. 1(g)]. Strong vibrational modes are observed in the Raman spectra, the most intense being the symmetrical ν_1 and asymmetrical ν_3 stretching modes, shown in Fig. 2(a). In phase I, these modes appear as a single broad band ($\sim 2250 \text{ cm}^{-1}$ at 2.5 GPa). The ν_2 molecular bending mode, observed at frequencies of $\sim 1010 \text{ cm}^{-1}$, is largely unaffected by pressure due to the “bent” molecular geometry. The behaviour of the vibrational Raman spectra of H_2Se is very similar to that of H_2S but shifted to lower frequencies. In phase I, the Raman frequencies of ν_1 and ν_3 of H_2Se differ by 300 cm^{-1} compared with the equivalent modes of H_2S , whilst the bending mode differs by 175 cm^{-1} (see Fig. 3).^{26,39} In all our experimental runs, H_2Se tended to form multiple single crystals (see the insets of Fig. 4); however, due to the sensitivity of the sample to synchrotron x-ray exposure, it was difficult to acquire data capable of completely refining a structure. Despite this, we were able to determine the structure of H_2Se at 4.1 GPa, confirming that H_2Se crystallizes into cubic phase-I [$Fm\bar{3}m$, $a = 5.424(3) \text{ \AA}$], shown in Fig. 4. The structure of phase I of H_2Se is equivalent to that of phase I of H_2S .¹⁸

At pressures of 7.7 GPa, the unresolved ν_1 and ν_3 modes begin to differ in intensity, with ν_1 being the more intense. This was determined previously for H_2S to indicate transformation to an intermediate phase I'.³⁹ Above pressures of 12 GPa, there is a further transformation to phase IV, characterised by the splitting of ν_1 and ν_3 , and from a reduction in peak width and increase in intensity. The asymmetrical stretching

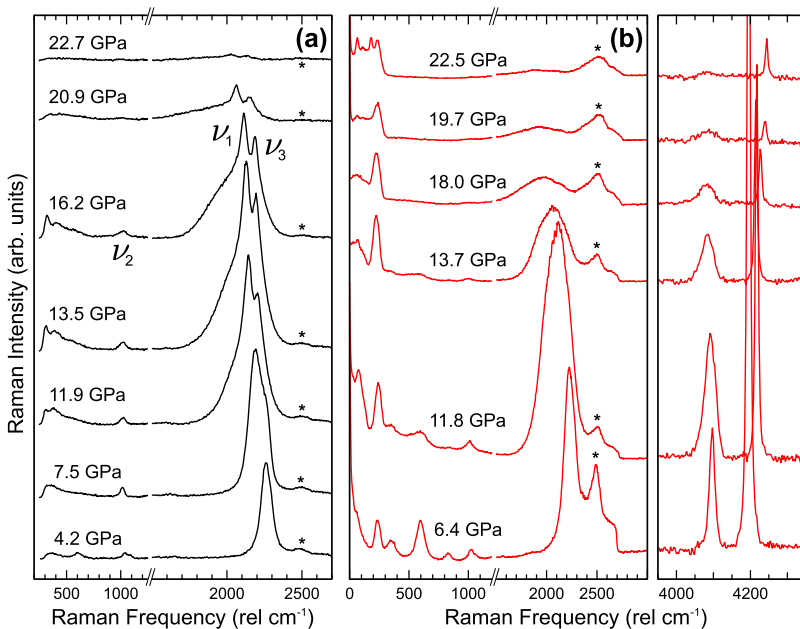


FIG. 2. (a) Representative Raman spectra of H_2Se on compression at 300 K (black). (b) Representative Raman spectra of $(\text{H}_2\text{Se})_2\text{H}_2$ formed from a H_2 -rich mixture at 300 K (red). The second order diamond is indicated by *.

mode, ν_3 , is higher in frequency by 860 cm^{-1} compared with ν_1 . Due to the instability of the sample to synchrotron x-ray exposure, we were unable to confirm a structural transition to phase I' or IV in H_2Se through x-ray diffraction analysis; however, the Raman characteristics of the transitions are identical to those observed in H_2S . On further compression above 20 GPa, we see the reduced intensity of all vibrational modes, and the crystallites visibly darken as H_2Se dissociates into its constituent elements. The decomposition is complete by 24 GPa, and at 30 GPa, the x-ray diffraction measurements showed only incommensurate monoclinic Se-IV, whilst Raman measurements showed only the characteristic Raman spectrum of Se and H_2 . In H_2S , the dissociation at 300 K occurs from ~ 27 –50 GPa,^{23,24} the onset being slightly higher than that observed here in H_2Se although over a much greater pressure range. Given the reduced $X\text{-H}$ bond strength, it is unsurprising that H_2Se decomposes at lower pressure and within a much smaller pressure range than H_2S ; hence, one would expect H_2Te to decompose at even lower pressure, if it can be stabilized at all at room temperature. This successive reduction of hydride decomposition pressure throughout group 16 reflects the trend observed in the hydrogen halides, where HCl is stable to at least 50 GPa, with HBr and HI decomposing at 42 GPa and 10 GPa, respectively.^{40–42}

In all sample concentrations we studied with excess H_2 , we observed partial or full formation of an $\text{H}_2\text{Se}\text{-H}_2$ compound above pressures of 4.2 GPa, which we identify as $(\text{H}_2\text{Se})_2\text{H}_2$. Full formation of H_2Se was observed in samples with high H_2 concentration, as demonstrated in our x-ray diffraction measurements [Fig. 2(b)]. The formation was initially identified through the appearance of a second vibrational mode assigned to H_2 within the newly formed compound [see Fig. 2(b)]. This mode is $\sim 100 \text{ cm}^{-1}$ lower in frequency compared with pure H_2 and has different frequency pressure dependence. The ν_1 and ν_3 modes of H_2Se also behave very differently in the compound than in H_2Se , whereby we observe no splitting at phase IV conditions, and the modes soften rapidly

with pressures above 12 GPa. These observations are very similar to the Raman characteristics for $(\text{H}_2\text{S})_2\text{H}_2$ above 17 GPa, which was synthesized in $\text{H}_2\text{S}\text{-H}_2$ mixtures.²⁷ To confirm that this is an analogous compound formed in $\text{H}_2\text{Se}\text{-H}_2$ mixtures, we have performed x-ray diffraction measurements (see Figs. 4 and 5). Due to the sample sensitivity to synchrotron x-ray exposure and propensity to form large single-crystal grains, it was difficult to collect high-quality diffraction patterns; however, we were able to obtain a sufficient number of reflections to allow indexing to a body-centered tetragonal structure, space group $I4/mcm$ with $a = 7.518(4)$ and $c = 6.266(4) \text{ \AA}$ at 5.2 GPa, and unit-cell dimensions could be extracted to 14.9 GPa (see Fig. 5). The significant diffuse scattering observed is strongly suggestive of hindered rotational disorder in the H_2Se molecules.⁴³

It is interesting that changes in volume per formula unit (V/Z) with pressure shows that $(\text{H}_2\text{Se})_2\text{H}_2$ adopts a volume marginally greater (3% on average) than the sum of its constituent elements [solid line in Fig. 5(b)]. This is an indication that $(\text{H}_2\text{Se})_2\text{H}_2$ is highly unstable, which is in agreement with our other observations. It is notable that the volume difference increases with pressure, reflecting the increased instability of $(\text{H}_2\text{Se})_2\text{H}_2$ relative to decomposition into Se and H_2 with increasing pressure. Similar behaviour is observed in pure H_2Se at pressure; at 4.1 GPa, we observe $V/Z = 39.887(4) \text{ \AA}^3$, while the volume calculated from the constituent elements is $V/Z = 37.321 \text{ \AA}^3$. This behaviour, although highly unusual, is not unique; recently we have reported on the equation of state of HI , another highly unstable compound under pressure, which appears to have an experimentally determined V/Z 7.3% greater than that calculated from I and H.⁴²

On compression, we do not see any evidence for further phase transitions in $(\text{H}_2\text{Se})_2\text{H}_2$, such as the ordering transition observed in $(\text{H}_2\text{S})_2\text{H}_2$. Instead, $(\text{H}_2\text{Se})_2\text{H}_2$ starts to decompose at exactly the same pressure conditions as H_2Se observing the reduced intensity of the vibrational modes. At pressures

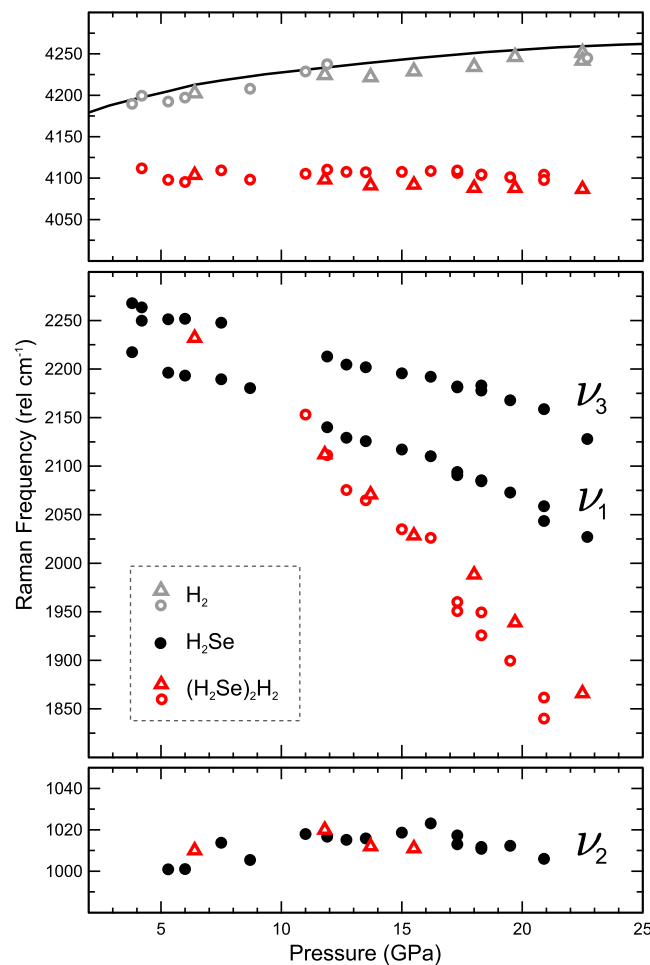


FIG. 3. Vibrational Raman frequencies of H_2Se (black closed circles), $(\text{H}_2\text{Se})_2\text{H}_2$ (red open circles/triangles), and H_2 (grey open circles/triangles) as functions of pressure. Filled circles, open circles, and open triangles correspond to different experimental runs. Top panel: Vibrational modes of excess hydrogen (grey symbols) and hydrogen molecules within $(\text{H}_2\text{Se})_2\text{H}_2$ (red). Solid black line corresponds to measurements of pure H_2 . Middle panel: Symmetrical, ν_1 , and asymmetrical, ν_3 , stretching modes of H_2Se (black) and the corresponding modes within $(\text{H}_2\text{Se})_2\text{H}_2$ (red). Bottom panel: The ν_2 molecular bending mode of H_2Se (black) and the corresponding mode within $(\text{H}_2\text{Se})_2\text{H}_2$ (red).

approaching 22.5 GPa, the sample visibly phase separates and the transparent $(\text{H}_2\text{Se})_2\text{H}_2$ crystals become dark and metallic, which shows the characteristic low frequency modes of Se [see Fig. 2(b)], with the remaining sample being transparent molecular hydrogen.

Recent x-ray synchrotron measurements have suggested that high- T_c superconducting H_2S could be due to the formation of H_3S , which reforms upon partial decomposition of H_2S at high pressure.^{8–10} Our study demonstrates that H_2Se and $\text{H}_2\text{Se}-\text{H}_2$ mixtures behave very similar to H_2S and $\text{H}_2\text{S}-\text{H}_2$ at high pressure and 300 K. Assuming the decomposition of H_2Se can be stabilized by low temperatures, it is very plausible that H_3Se is formed at high pressures; if H_3S is indeed the thermodynamically stable high pressure phase of H_2S . Given that the behaviour of H_2S above 100 GPa is not completely understood,^{2–10} experiments on H_2Se at the conditions in which superconductivity is predicted could prove very insightful for all the hydrogen chalcogenides.

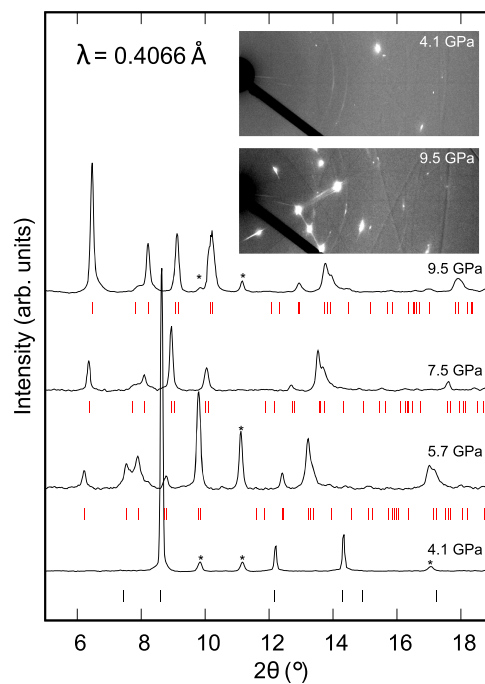


FIG. 4. X-ray diffraction data for H_2Se and $(\text{H}_2\text{Se})_2\text{H}_2$ at high pressures. Below 4.1 GPa, diffraction spots due to phase-I of H_2Se are observed (black tick marks). Above 4.1 GPa, diffraction spots corresponding to the hydrogen-bonded compound $(\text{H}_2\text{Se})_2\text{H}_2$ are observed up to pressures of 14.9 GPa (red tick marks). Peaks marked with (*) are due to the Re gasket. Inset: Single crystal-like x-ray diffraction patterns of H_2Se at 4.1 GPa and $(\text{H}_2\text{Se})_2\text{H}_2$ at 9.5 GPa, the latter of which includes significant streaks of diffuse scattering.

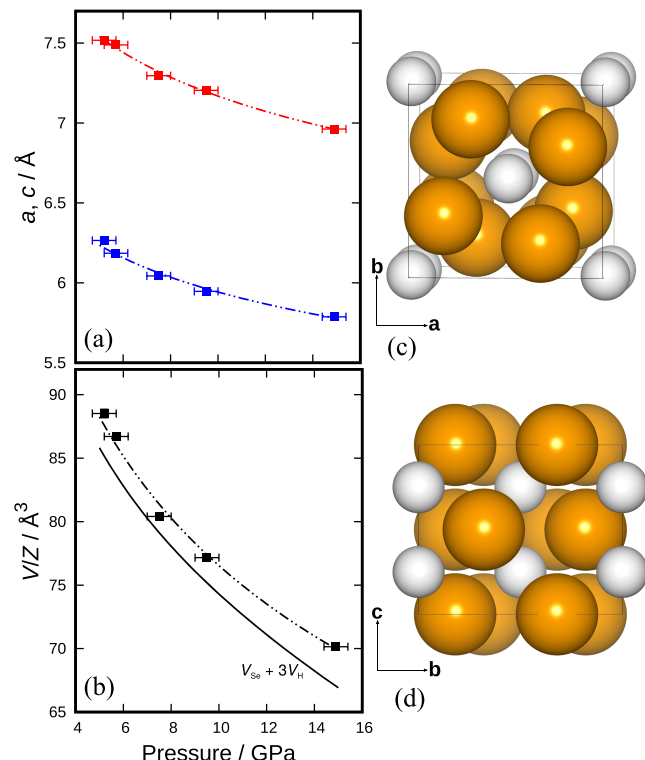


FIG. 5. (a) Changes in unit-cell dimensions for $(\text{H}_2\text{Se})_2\text{H}_2$ as a function of pressure (a —red and c —blue). (b) V/Z as a function of pressure for $(\text{H}_2\text{Se})_2\text{H}_2$. The solid line indicates volume calculated according to the atomic equations of state for H_2 ³⁷ and Se.³⁸ [(c) and (d)] Structure of $(\text{H}_2\text{Se})_2\text{H}_2$ viewed down the c and a axes illustrating the layered nature of the compound.

ACKNOWLEDGMENTS

This work was supported by a research grant from the UK Engineering and Physical Sciences Research Council. Portions of this work were performed at HPCAT (Sector 16), Advanced Photon Source (APS), Argonne National Laboratory. HPCAT operations are supported by DOE-NNSA under Award No. DE-NA0001974, with partial instrumentation funding by NSF. The Advanced Photon Source is a U.S. Department of Energy (DOE) Office of Science User Facility operated for the DOE Office of Science by Argonne National Laboratory under Contract No. DE-AC02-06CH11357. The authors thank Ross Hrubiak for his assistance.

- ¹A. P. Drozdov, M. I. Eremets, I. A. Troyan, V. Ksenofontov, and S. I. Shylin, *Nature* **525**, 73 (2015).
- ²A. F. Goncharov, S. S. Lobanov, V. B. Prakapenka, and E. Greenberg, *Phys. Rev. B* **95**, 140101 (2017).
- ³B. Guigue, A. Marizy, and P. Loubeyre, *Phys. Rev. B* **95**, 020104(R) (2017).
- ⁴I. Troyan, A. Gavriluk, R. Rüffer, A. Chumakov, A. Mironovich, I. Lyubutin, D. Perekalin, A. P. Drozdov, and M. I. Eremets, *Science* **351**, 1303 (2016).
- ⁵E. E. Gordon, K. Xu, H. Xiang, A. Bussmann-Holder, R. K. Kremer, A. Simon, J. Köhler, and M. H. Whangbo, *Angew. Chem., Int. Ed.* **55**, 3682 (2016).
- ⁶I. Errea, M. Calandra, C. J. Pickard, J. R. Nelson, R. J. Needs, Y. Li, H. Liu, Y. Zhang, Y. Ma, and F. Mauri, *Nature* **532**, 81 (2016).
- ⁷R. Akashi, W. Sano, R. Arita, and S. Tsuneyuki, *Phys. Rev. Lett.* **117**, 075503 (2016).
- ⁸M. Einaga, M. Sakata, T. Ishikawa, K. Shimizu, M. I. Eremets, A. P. Drozdov, I. A. Troyan, N. Hirao, and Y. Ohishi, *Nat. Phys.* **12**, 835 (2016).
- ⁹A. F. Goncharov, S. S. Lobanov, I. Kruglov, X.-M. Zhao, X.-J. Chen, A. R. Oganov, Z. Konôpková, and V. B. Prakapenka, *Phys. Rev. B* **93**, 174105 (2016).
- ¹⁰Y. Li, L. Wang, H. Liu, Y. Zhang, J. Hao, C. J. Pickard, J. R. Nelson, R. J. Needs, W. Li, Y. Huang, I. Errea, M. Calandra, F. Mauri, and Y. Ma, *Phys. Rev. B* **93**, 020103 (2016).
- ¹¹S. Zhang, Y. Wang, J. Zhang, H. Liu, X. Zhong, H.-F. Song, G. Yang, L. Zhang, and Y. Ma, *Sci. Rep.* **5**, 15433 (2015).
- ¹²X. Zhong, H. Wang, J. Zhang, H. Liu, S. Zhang, H.-F. Song, G. Yang, L. Zhang, and Y. Ma, *Phys. Rev. Lett.* **116**, 057002 (2016).
- ¹³G. Natta, *Nature* **127**, 129 (1931).
- ¹⁴J. H. Loehlin, P. G. Mennitt, and J. S. Waugh, *J. Chem. Phys.* **44**, 3912 (1966).
- ¹⁵Z. M. E. Saffar and P. Schultz, *J. Chem. Phys.* **56**, 2524 (1972).
- ¹⁶B. A. Paldus, S. A. Schlueter, and A. Anderson, *J. Raman Spectrosc.* **23**, 87 (1992).
- ¹⁷J. A. Flores-Livas, A. Sanna, and E. K. U. Gross, *Eur. Phys. J. B* **89**, 63 (2016).
- ¹⁸J. K. Cockcroft and A. N. Fitch, *Z. Kristallogr.* **193**, 1 (1990).
- ¹⁹H. Fujihisa, H. Yamawaki, M. Sakashita, K. Aoki, S. Sasaki, and H. Shimizu, *Phys. Rev. B* **57**, 2651 (1998).
- ²⁰S. Endo, A. Honda, K. Koto, O. Shimomura, T. Kikegawa, and N. Hamaya, *Phys. Rev. B* **57**, 5699 (1998).
- ²¹J. S. Loveday, R. J. Nelmes, S. Klotz, J. M. Besson, and G. Hamel, *Phys. Rev. Lett.* **85**, 1024 (2000).
- ²²R. Rousseau, M. Boero, M. Bernasconi, M. Parrinello, and K. Terakura, *Phys. Rev. Lett.* **85**, 1254 (2000).
- ²³H. Fujihisa, H. Yamawaki, M. Sakashita, A. Nakayama, T. Yamada, and K. Aoki, *Phys. Rev. B* **69**, 214102 (2004).
- ²⁴M. Sakashita, H. Yamawaki, H. Fujihisa, K. Aoki, S. Sasaki, and H. Shimizu, *Phys. Rev. Lett.* **79**, 1082 (1997).
- ²⁵S. Endo, A. Honda, S. Sasaki, H. Shimizu, O. Shimomura, and T. Kikegawa, *Phys. Rev. B* **54**, R717 (1996).
- ²⁶H. Shimizu, Y. Nakamichi, and S. Sasaki, *J. Chem. Phys.* **95**, 2036 (1991).
- ²⁷T. A. Strobel, P. Ganesh, M. Somayazulu, P. R. C. Kent, and R. J. Hemley, *Phys. Rev. Lett.* **107**, 255503 (2011).
- ²⁸Y. Li, J. Hao, H. Liu, Y. Li, and Y. Ma, *J. Chem. Phys.* **140**, 174712 (2014).
- ²⁹D. Duan, Y. Liu, F. Tian, D. Li, X. Huang, Z. Zhao, H. Yu, B. Liu, W. Tian, and T. Cui, *Sci. Rep.* **4**, 6968 (2014).
- ³⁰H. K. Mao, J. Xu, and P. M. Bell, *J. Geophys. Res.* **91**, 4673, doi: 10.1029/jb091ib05p04673 (1986).
- ³¹P. Dalladay-Simpson, R. T. Howie, and E. Gregoryanz, *Nature* **529**, 63 (2016).
- ³²R. T. Howie, R. Turnbull, J. Binns, M. Frost, P. Dalladay-Simpson, and E. Gregoryanz, *Sci. Rep.* **6**, 34896 (2016).
- ³³C. Prescher and V. B. Prakapenka, *High Pressure Res.* **35**, 223 (2015).
- ³⁴B. H. Toby and R. B. Von Dreele, *J. Appl. Crystallogr.* **46**, 544 (2013).
- ³⁵A. Le Bail, H. Duroy, and J. Fourquet, *Mater. Res. Bull.* **23**, 447 (1988).
- ³⁶V. Petříček, M. Dušek, and L. Palatinus, *Z. Kristallogr. - Cryst. Mater.* **229**, 345 (2014).
- ³⁷P. Loubeyre, R. LeToullec, D. Hausermann, M. Hanfland, R. J. Hemley, H. K. Mao, and L. W. Finger, *Nature* **383**, 702 (1996).
- ³⁸M. I. McMahan, C. Hejny, J. S. Loveday, and L. F. Lundegaard, *Phys. Rev. B* **70**, 054101 (2004).
- ³⁹H. Shimizu, H. Yamaguchi, S. Sasaki, A. Honda, S. Endo, and M. Kobayashi, *Phys. Rev. B* **51**, 9391 (1995).
- ⁴⁰E. Katoh, H. Yamawaki, H. Fujihisa, M. Sakashita, and K. Aoki, *Phys. Rev. B* **59**, 11244 (1999).
- ⁴¹T. Kume, T. Tsuji, S. Sasaki, and H. Shimizu, *Phys. Rev. B* **58**, 8149 (1998).
- ⁴²J. Binns, X.-D. Liu, P. Dalladay-Simpson, V. Afonina, E. Gregoryanz, and R. T. Howie, *Phys. Rev. B* **96**, 144105 (2017).
- ⁴³J. Binns, G. J. McIntyre, J. A. Barreda-Argüeso, J. González, F. Aguado, F. Rodríguez, R. Valiente, and S. Parsons, *Acta Crystallogr., Sect. B: Struct. Sci., Cryst. Eng. Mater.* **73**, 844 (2017).